AIAA JOURNAL
Vol. 42, No. 12, December 2004

Technical Notes

TECHNICAL NOTES are short manuscripts describing new developments or important results of a preliminary nature. These Notes cannot exceed six manuscript pages and three figures; a page of text may be substituted for a figure and vice versa. After informal review by the editors, they may be published within a few months of the date of receipt. Style requirements are the same as for regular contributions (*see inside back cover*).

Effects of Boundary-Layer Velocity Fluctuations on Unsteadiness of Blunt-Fin Interactions

Y. X. Hou,* Ö. H. Ünalmis,† P. C. Bueno,*
N. T. Clemens,‡ and D. S. Dolling§
University of Texas at Austin, Austin, Texas 78712-1085

Introduction

EXPERIMENTS from a wide range of test facilities, from continuous to intermittent, from transonic to hypersonic, have shown that shock-induced turbulent boundary-layer separation is a highly unsteady process.[1,2] Most studies of interaction unsteadiness have been concerned with characterizing the unsteadiness of the separation shock, or in particular, the separation shock "foot," defined as the portion of the separation shock closest to the wall. The unsteady motion of the separation shock foot is characterized by a wide range of frequencies, typically of order a few hundred hertz to several kilohertz. In the laboratory the upper limit of this range can be an order of magnitude smaller than the frequencies that characterize the large-scale structures of the upstream boundary layer. Nevertheless, it has been suggested that that the highest-frequency shock-foot motions are driven by fluctuations in the upstream boundary layer, whereas the lower frequencies are driven by low-frequency pulsations of the separated flow region.[3]

There is currently no consensus on the physical mechanism that drives the low-frequency unsteadiness, but recent progress has been made in this regard. In particular, Beresh et al.[4] used particle image velocimetry (PIV) to investigate the role of upstream boundary-layer velocity fluctuations on the separation shock-foot motion in a Mach 5 compression ramp interaction. They made PIV measurements in the upstream boundary layer, while monitoring the shock-foot location by using several fast-response pressure transducers located under the intermittent region. The intermittent region is defined as the streamwise distance over which shock-foot motion occurs. Beresh et al. conditionally averaged their data based on different types of shock-foot motions to determine if certain motions were correlated with particular types of boundary-layer fluctuations. Their results showed that the positive streamwise velocity fluctuations in the lower part of the upstream boundary layer were correlated with downstream shock-foot motions, and negative velocity fluctuations were correlated with upstream shock foot motions. They concluded that these results were consistent with the simple physical principle that a fuller upstream velocity profile provides increased resistance to separation and thus results in downstream shock motion. By the same argument, a less-full velocity profile results in upstream motion of the shock foot. They further showed that the maximum correlations between upstream fluctuations and shock-foot motion were obtained at frequencies that were significantly lower than the characteristic frequencies of the large-scale structures in the boundary layer. This indicates that the fluctuations responsible for driving the separated flow are at the low end of the turbulence energy spectrum or are not caused by turbulence at all, but perhaps to some type of low-frequency fluctuations associated with the wind tunnel itself. For instance, there exists evidence that wind-tunnel noise affects the pressure fluctuations measured under attached turbulent boundary layers,[5] and thus it is possible that noise influences the unsteadiness of shock-induced turbulent separation.

Regardless of the source of the upstream perturbations, an important question to ask is whether the mechanism identified in Ref. 4 is a universal one, that is, does it apply across the wide range of shock-induced turbulent separated flows or is it particular (or singularly dominant) to two-dimensional interactions such as those generated by unswept compression ramps? It is well known that there are fundamental differences in the scaling of unsteady turbulent boundary-layer separation induced by compression ramps and blunt fins. In the former, the intermittent region scales on δ_0 (the 99% velocity thickness of the incoming boundary layer), whereas in the latter case it scales on the fin diameter D. The implication of this is that in compression ramp flows the intermittent region is limited to about a boundary-layer thickness in length, whereas in the fin-induced interaction it can be tens of boundary-layer thicknesses in extent. The blunt-fin flowfield is characterized by an unsteady shock foot that wraps around the fin leading edge. Beneath this foot, the boundary layer separates, and a complex horseshoe vortex system develops. This vortex system wraps about the fin root and trails downstream.[6–8] Because the blunt-fin interaction scales with the fin geometry rather than the upstream boundary-layer thickness, it is possible that its unsteady characteristics might also be insensitive to the upstream boundary layer. The blunt fin is therefore an ideal flow for testing the universality of the mechanism found to apply in unswept compression ramp interactions.[4]

Experimental Program

All of the experiments were conducted in the Mach 5 blowdown tunnel of the University of Texas at Austin. The constant-area test section was 15.2 cm wide by 17.8 cm high and had a length of 76.2 cm. The stagnation pressure and temperature were $P_0 = 2.24$ MPa and $T_0 = 353$ K; the freestream Mach number, velocity, and unit Reynolds number were $M_\infty = 4.95$, $U_\infty = 765$ m/s, and $Re_\infty = 5.0 \times 10^7$ m^{-1}; and the upstream boundary-layer thickness was $\delta_0 = 1.93$ cm.

A hemicylindrically blunted fin with leading-edge diameter of $D = 1.91$ cm and a height of 10.16 cm ($\approx 5\delta_0$) was used to generate

Presented as Paper 2000-2450 at the AIAA 21st Aerodynamic Measurement Technology and Ground Testing Conference, Denver, CO, 19–22 June 2000; received 20 May 2004; revision received 7 July 2004; accepted for publication 21 July 2004.

*Graduate Student, Center for Aeromechanics Research, Department of Aerospace Engineering and Engineering Mechanics. Student Member AIAA.

†Research Associate, Center for Aeromechanics Research, Department of Aerospace Engineering and Engineering Mechanics; currently Flow Engineer, Weatherford/eProduction Solutions, Inc., 22001 North Park Drive, Kingwood, TX 77339. Senior Member AIAA.

‡Associate Professor, Center for Aeromechanics Research, Department of Aerospace Engineering and Engineering Mechanics; clemens@mail.utexas.edu. Associate Fellow AIAA.

§Professor, Center for Aeromechanics Research, Department of Aerospace Engineering and Engineering Mechanics. Fellow AIAA.

the separated flow (Fig. 1). The instantaneous location of the shock foot was determined by using a row of five fast-response pressure transducers (Kulite model XCQ-062-50A or XCQ-062-15A) flush mounted under the intermittent region. The spacing between transducers was 2.9 mm. The transducers had a pressure-sensitive diaphragm of 0.71 mm in diameter, and their frequency response was 50 kHz. This provided sufficient resolution because the characteristic frequency of the large-scale boundary-layer structures is of order U_∞/δ_0, which corresponds to a frequency of about 40 kHz. The pressure data were low-pass filtered (cutoff frequency 40 kHz) and then digitized at the rate of 100 kHz. For pressure-only measurements 262,144 data points per channel were acquired, whereas records of 4096 data points per channel were acquired for the simultaneous pressure and PIV measurements. Pretriggering of the A/D converter enabled the acquisition of the PIV images at the center of each 4096-point pressure-data record.

The PIV image acquisition system used in the current study is shown in Fig. 2. The light source of the system was a dual-cavity Nd:YAG laser (Spectra-Physics PIV-400), which provided two pulses, each with energy of 55 mJ, and with temporal separation of 1 μs. The scattering from the seeded particles was detected with a 1k × 1k pixel, frame-straddling, charge-coupled-device camera (Kodak ES 1.0). The particles used were aluminum oxide (Al_2O_3) with a manufacturer's specification of 0.3-μm diam and were delivered using a two-stage fluidized-bed seeder. The particles were introduced into the test section through a streamlined injector, which was installed on the test-section floor well upstream of the blunt fin (71 cm) to allow the boundary layer to recover from the disturbance. The injector had a tapered diamond shape and was 1.52 cm high × 1.4 cm wide × 10.9 cm long (in the streamwise direction). To assess the potential interference of the injector on the interaction region, fluctuating pressure measurements were made with and without the injector in place. Figure 3 shows the normalized power spectra of the signals recorded by the third upstream transducer for two different cases: 1) undisturbed flow, with no injector in place, and 2) disturbed flow with injector in place and particle injection. The figure shows that the power spectrum for the disturbed case agrees well with that of the undisturbed case and indicates that the injector does not have a significant effect on the dynamics of the flow in the interaction region.

More than 4000 PIV image pairs were acquired in the current study to enable conditional averaging of the PIV data. The PIV

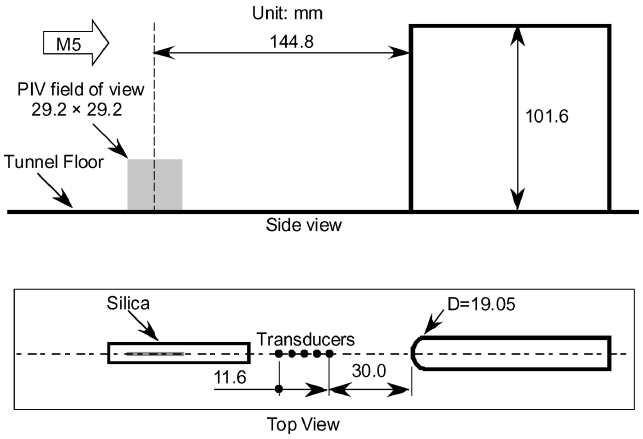

Fig. 1 Schematic diagram of the blunt-fin model mounted in the Mach 5 wind-tunnel test section. The PIV measurements were made along the tunnel centerline, 145 mm upstream of the fin leading edge. A streamwise row of flush-mounted pressure transducers enabled the detection of the shock-foot location.

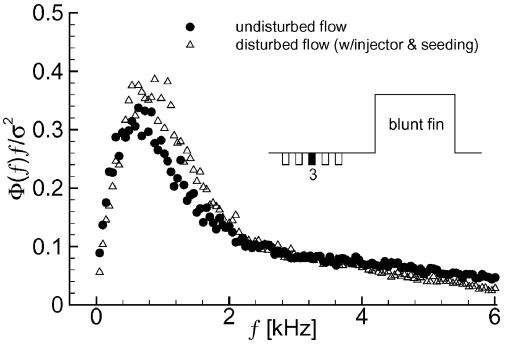

Fig. 3 Effect of the PIV seed-particle injector on the pressure power spectral density measured at transducer 3. The spectra have been normalized by the rms pressure σ.

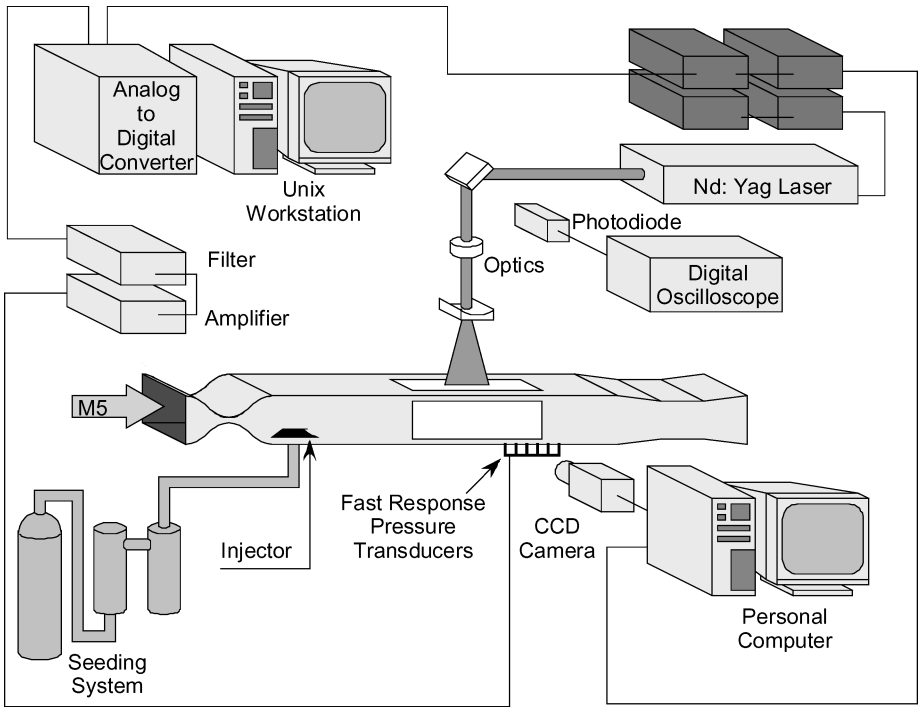

Fig. 2 Schematic diagram of the experimental setup for simultaneous PIV and fast-response pressure measurements in a Mach 5 blunt-fin-induced interaction.

processing interrogation window was 32×32 pixels (no overlap), which resulted in 32×32 vector fields corresponding to a resolution in the flow of about 1×1 mm. Further details of the experimental setup, pressure data acquisition system, PIV system, and data processing can be found in Refs. 4 and 9.

Results and Discussion

The same analysis approach as Beresh et al.[4] was adopted for the present blunt-fin-induced interaction. The PIV vector fields were sorted into five different groups that depended on the nature of the shock-foot motion that occurred within a time window just after the PIV image was acquired. The groups were for upstream and downstream motions of one and two transducer spacings, and no motion at all, during the time window. Only unidirectional shock motions during the time window were used because it was believed that such motions would exhibit a stronger correlation, if present.

Conditional ensemble-average profiles of the streamwise velocity fluctuations $\bar{u}'(y)$ were acquired for three different time windows of 100, 250, and 500 μs, which correspond to acquisition bandwidths of 10, 4, and 2 kHz, respectively. Note that the quantity $\bar{u}'$ is the mean of the fluctuating velocity (not the rms value), and so by definition will average to zero when the averaging process is unconditional. Transverse profiles of the conditional ensemble-average velocity fluctuations for a time window corresponding to 10 kHz are shown in Fig. 4. The numbers in parentheses in the legend of Fig. 4 denote the number of PIV images (vector fields) included in the ensemble averaging. Each PIV vector field had a resolution of 32×32 vectors, and each ensemble average was computed by averaging across each row of the vector fields (i.e., for an ensemble of N vector fields, averages were computed using $32N$ data points). The error bars represent 95%-confidence precision-uncertainty levels and were estimated based on a statistical analysis of the data. Figure 4 shows a profile (labeled "unconditional") that corresponds to the unconditional mean of the u' velocity fluctuations and which should be zero at all transverse locations. In fact, when the unconditional mean is computed from all 4093 PIV vector fields, it is identically zero at all y locations as expected. The reason only 450 vector fields were used in the unconditional mean is to give the reader an idea of the magnitude of the statistical variations that are associated with the finite sample sizes used for the conditional averages.

The conditional profiles shown are averages of u' that have been conditioned upon the following types of shock motion: shock stationary, upstream motion of one bin and two bins, and downstream motion of one bin and two bins, where a bin corresponds to the spacing between adjacent pressure transducers (=2.9 mm). For example, the shock-foot-stationary profile is essentially zero at all transverse locations. This means that for instances when the shock foot does not move in the 100 μs (10 kHz) time window, then the upstream boundary-layer velocity fluctuations that convect into the interaction during this time window tend to average to zero. Furthermore, it is seen from Fig. 4 that all of the profiles are essentially zero for $y > 5$ mm, which implies that the shock motion is not correlated with any particular type of velocity fluctuations in the outer part of the upstream boundary layer. It is also seen, however, that in the lower part of the boundary layer there is a significant correlation between the velocity fluctuations and the specific types of shock-foot motions. In particular, for $y < 5$ mm upstream motions of one bin and two bins tend to be correlated with the ensemble-average velocity fluctuations of about -10 and -25 m/s, respectively. The opposite trend is seen for downstream shock motions, that is, motions of one bin and two bins downstream are correlated with mean fluctuations of 5 and 10 m/s, respectively. The unconditional fluctuations average to zero, and so these results indicate a systematic trend.

Another interesting feature of Fig. 4 is that it shows that there is an asymmetry in the magnitude of the fluctuations for upstream and downstream shock-foot motion. In other words, the fluctuations that are correlated with downstream motion are smaller than those that are correlated with upstream motion. This trend was also observed in the previous compression-ramp study.[4] One interpretation of this asymmetry is that there is a higher resistance to upstream motion of the shock foot, and therefore larger magnitude velocity fluctuations are required to move it. This might also explain why the stationary case is correlated with slightly negative fluctuations; that is, the shock-foot has a tendency to move downstream and so larger fluctuations are required to keep it stationary. (Note that the stationary case was computed from a large sample set, and so the trend seen near the wall is larger than the precision uncertainty.)

The profiles of the ensemble-average velocity fluctuations for a time window corresponding to 4 and 2 kHz were also computed (not shown). When compared to the 10-kHz window, the trend for the 4-kHz window for the blunt fin is similar, although the data are not as well converged because of the smaller sample sizes owing to the lower probability of unidirectional motion in a 250-μs time window.[9] In contrast to the shorter time windows, the 2-kHz case shows no significant correlation of velocity fluctuations with shock motion. This is in agreement with the compression ramp case, where the correlations for 2-kHz window were also significantly reduced.[4]

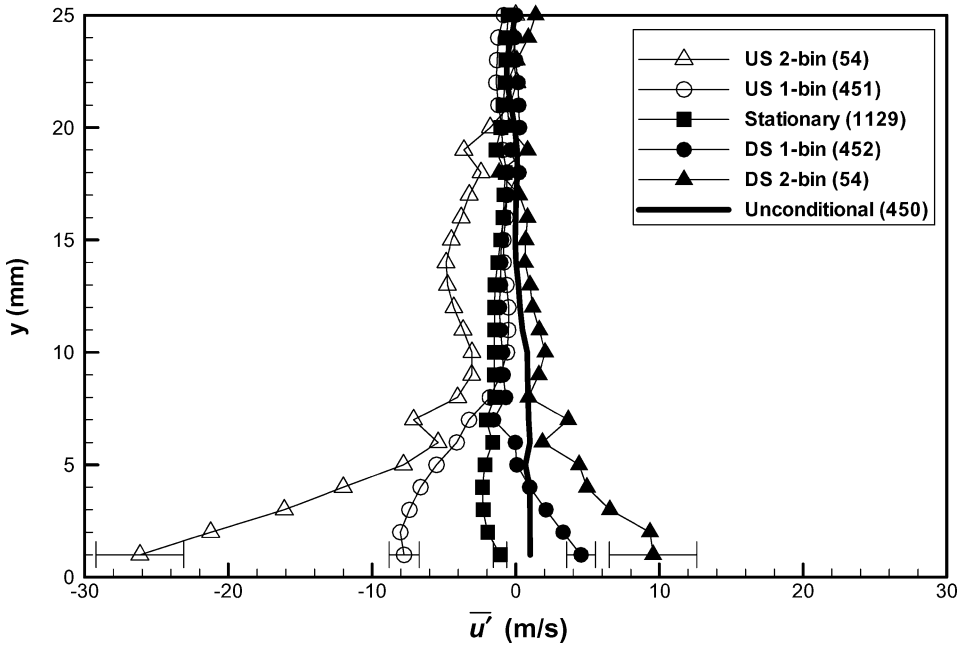

Fig. 4 Conditional ensemble-average profiles of the streamwise velocity fluctuations in the incoming boundary layer conditioned upon the separation shock-foot motion within a time period of 100 μs (corresponding to a frequency of 10 kHz).

The correlations seen in the blunt-fin case are qualitatively similar to those obtained in compression ramp flows,[4] namely, negative velocity fluctuations in the lower part of the incoming boundary layer correlate with upstream shock motions and vice versa. In the current study the strongest correlations were associated with a detection bandwidth of 10 kHz, whereas in the compression ramp interaction (which was generated in the same wind tunnel) the strongest correlations occurred at 4 kHz (Ref. 4). Because the large-scale structures in the outer part of the boundary layer have a characteristic frequency of order $U_\infty/\delta_0 = 40$ kHz, the source of the velocity fluctuations is likely not these outer-scale structures. In Ref. 4 it is suggested that the velocity fluctuations might be associated with the low-frequency end of the turbulence energy spectrum, or perhaps even some nonturbulent mechanism such as Göertler vortices that are generated by the concave curvature of the nozzle. Furthermore, as mentioned earlier, wind-tunnel noise has been shown to affect the pressure fluctuations in turbulent boundary layers[5] and so an aeroacoustic source for the velocity fluctuations, which might be geometry dependent, cannot be ruled out.

Although the source of the fluctuations is not known, Fig. 4 shows that the magnitude of the velocity fluctuations that correlate with the larger-scale shock motions is about 10–30 m/s. (Note that it is entirely possible that the fluctuations could continue to increase closer to the wall.) Interestingly, the magnitude of these fluctuations is about 2–4% of the freestream velocity, which is of the same order of magnitude as the mean shock velocity measured in a range of different interactions including swept and unswept compression ramps and blunt fins.[10]

Finally, it is also interesting to consider the present results in the light of the work of Gonsalez and Dolling,[10] who showed that the mean and rms shock speed are essentially constant irrespective of model geometry and intermittent region length. They also showed that the separation shock Strouhal number defined using intermittent region length, maximum shock zero crossing frequency, and freestream velocity is essentially constant. The fact that some of the separation shock characteristics appear to be insensitive to the downstream flowfield/model geometry lends implicit support to the idea that forcing by the upstream boundary layer plays a more significant role in the separation shock unsteadiness than the downstream effects.

Summary

In conclusion, taken as a whole, these results suggest that shock-foot unsteadiness in compression ramp[4] and the blunt-fin interactions, whose mean flow structures are quite different and whose mean length scales depend on different parameters, exhibit strong similarities. These similarities further suggest the basic mechanisms that drive the unsteadiness of interactive flows might be universal and fundamentally tied to forcing by the upstream boundary layer.

Acknowledgments

Support for this research has been provided through Grants DAAG55-98-1-0062 and DAAG55-98-1-0290 from the Army Research Office monitored by T. Doligalski. The authors gratefully acknowledge this support.

References

[1]Dolling, D. S., "50 Years of Shock-Wave/Boundary Layer Interaction Research: What Next?," *AIAA Journal*, Vol. 39, No. 8, 2001, pp. 1517–1531.

[2]Smits, A. J., and Dussuage, J. P., *Turbulent Shear Layers in Supersonic Flow*, AIP Press, New York, 1996, pp. 285–319.

[3]Erengil, M. E., and Dolling, D. S., "Physical Causes of Separation Shock Unsteadiness in Shock Wave/Turbulent Boundary-Layer Interactions," AIAA Paper 93-3134, July 1993.

[4]Beresh, S. J., Clemens, N. T., and Dolling, D. S., "Relationship Between Upstream Turbulent Boundary-Layer Velocity Fluctuations and Separation Shock Unsteadiness," *AIAA Journal*, Vol. 40, No. 12, 2002, pp. 2412–2422.

[5]Beckwith, I. E., "Development of a High Reynolds Number Quiet Wind Tunnel for Transition Research," *AIAA Journal*, Vol. 13, No. 3, 1975, pp. 300–306.

[6]Kaufman, L. G., II, Korkegi, R. H., and Morton, L. C., "Shock Impingement Caused by Boundary Layer Separation Ahead of Blunt Fins," *AIAA Journal*, Vol. 11, No. 10, 1973, pp. 1363, 1364.

[7]Saida, N., and Hattori, H., "Shock Wave-Turbulent Boundary Layer Interactions Induced by a Blunt Fin," *Transactions of the Japan Society for Aeronautical and Space Science*, Vol. 27, No. 76, 1984, pp. 67–77.

[8]Fomison, N. R., and Stollery, J. L., "The Effects of Bluntness on a Glancing Shock Wave Turbulent Boundary Layer Interaction," AGARD CP 428, 1987.

[9]Ünalmis, Ö. H., Hou, Y. X., Bueno, P. C., Clemens, N. T., and Dolling, D. S., "PIV Investigation of Role of Boundary Layer Velocity Fluctuations in Unsteady Shock-Induced Separation," AIAA Paper 2000-2450, June 2000.

[10]Gonsalez, J. C., and Dolling, D. S., "Correlation of Interaction Sweepback Effects on the Dynamics of Shock-Induced Turbulent Separation," AIAA Paper 93-0776, Jan. 1993.

H. Reed
Associate Editor